Supplementary Information for

Slow Cooling and Efficient Extraction of Hot Carriers in Perovskite Films via Engineering Trap-Mediated Relaxation Channel

Xinlei Zhang,[a,b] Jing Leng,*[b] Qi Sun,[b] Qingshun Dong,[b] Xinyu Tong,[b] Yu Song,[a] Yan Xu,*[a] Shengye Jin*[b] and Wenming Tian*[b]

[a] Department of Chemistry, College of Sciences, Northeastern University, Shenyang 110819, China

[b] State Key Laboratory of Chemical Reaction Dynamics, Dalian Institute of Chemical Physics, Chinese Academy of Sciences, Dalian 116023, China

Experimental method

Materials.

Formamidinium iodine (FAI, Advanced Election Technology CO., Ltd, 99.9%), Methylammonium iodide (MAI, Xi'an Polymer, 99.5%), Methyl ammonium chloride (MACl, Greatcell Solar, 99.9%), lead (II) iodide (PbI_2, Xi'an p-OLED Corp., 99.99%), ZnSe (Macklin, 99.99%), SnO_2 (Alfa, 15 wt %), N,N-dimethyformamide (DMF, Sigma-Aldrich, 99.9%), dimethyl sulfoxide (DMSO, Sigma-Aldrich, 99.9%), acetone (Kermel, 99.8%), ethanol (Sinopharm Chemical Reagent, 99%), isopropyl alcohol (IPA, Aladdin, 99.5%). All solvents and chemicals were purchased from a commercial company and directly used without further purification.

Preparation of $FAPbI_3$ films.

Glass slides (2 × 2 cm) were cleaned using an ultra-sonication bath in soap water and rinsed progressively with distilled water, isopropyl alcohol and acetone, and finally treated with oxygen plasma for 20 min. 90 mg FAI and 9 mg MACl were dissolved in 1 mL isopropanol solution, stirred at room temperature until dissolved in an N_2-filled glovebox. 1.5 M PbI_2 powder was dissolved in 1 mL DMF and DMSO (9:1, volume/volume), with stirring at 60 °C for 2 h in an N_2-filled glovebox. The PbI_2 precursor solution was spin-coated on the substrates at 2000 rpm for 30 s in the N_2-filled glovebox, annealed at 70 ℃ for 1 minutes. Then the FAI precursor solution was spin-coated on the PbI_2 thin films at 2000 rpm for 30 s, and then subjected to a 150 ℃ annealing for 15 minutes to form the $FAPbI_3$ perovskite thin films.

Preparation of Electron acceptor films

During the preparation of commercial SnO_2 thin films, the commercially purchased SnO_2 was mixed with deionized water according to the volume ratio of 1:3, and the mixed solution was oscillated for 1min to obtain the SnO_2 aqueous solution needed for our experiment. SnO_2 solution was spin-coated onto clean glass slides at 3000 rpm for 30 s and then annealed, yielding the resultant film with an electron acceptor.

During the preparation of ZnSe thin films, the pressure in the evaporation chamber

was set to about 10^{-4} Pa. The well-known "Edwards-E306A" coating device was equipped with a quartz crystal monitor (FTM4, Edwards, UK), which was used to monitor and control the deposition rate and simultaneously measure the thickness of the studied film. The final thickness of ZnSe is about 20 nm.

During the preparation of atomic layer-deposited (ALD) SnO_2 thin films, SnO_2 layers were grown directly on clean Glass slides. 220 ALD cycles were carried out, corresponding to an expected thickness of 22 nm.

Ultrafast TA spectroscopy measurement.

The femtosecond TA spectrometer is based on a Yb:KGW laser system (1030 nm, 100 kHz; Light Conversion Ltd.), nonlinear frequency mixing techniques and the Femto-TA100 spectrometer (Time-Tech Spectra LLC). Briefly, the 1030 nm output pulse from the regenerative amplifier was split in two parts. The transmitted part was used to pump a noncollinear Optical Parametric Amplifier (OPA) which generates a certain wavelength as pump beam. The other part was attenuated with a neutral density filter and focused into a YAG crystal to generate a white light continuum (WLC) from 550 nm to 950 nm used for probe beam. The probe beam was focused with a parabolic reflector onto the sample. After passing through the sample, the probe beam was collimated and then focused into a fiber-coupled spectrometer equipped with CMOS sensors. The intensity of the pump pulse used in the experiment was controlled by a variable neutral-density filter wheel. The delay between the pump and probe pulses was controlled by a motorized delay stage. The pump pulses were chopped by a synchronized chopper at 5 KHz and the absorbance change was calculated with two adjacent probe pulses (pump-blocked and pump-unblocked). All experiments were performed at room temperature.

Structural and spectral characterization of perovskite films.

The UV-vis absorption spectra of all samples were obtained using a Cary 60 UV-vis spectrometer of Agilent. The typical scanning electron microscope (SEM) and the element mapping images of $FAPbI_3$ film was measured by a JSM-7800F. The XRD

spectra were obtained on an X'pert Pro-1. Ultraviolet Photoelectron Spectroscopy (UPS) were obtained by a PHI 5000 Versaprobe III. The volumetric heat capacity of the perovskite films was measured using a Hot Disk Thermal Constants Analyzer (Thermometric AB, Sweden), employing the transient plane source (TPS) technique.

Carrier temperature fitting

For carriers distributed across the high-energy region, a rigorous Fermi-Dirac distribution defined by carrier temperature T_c can be approximated by a Maxwell-Boltzmann distribution, as shown in the Equation 1. The second term in that equation represents the photon-induced absorbance (PIA) in a parabolic band approximation. This equation is then fitted to a high energy tail of bleaching spectrum to extract the carrier temperature.

$$\Delta A(E) = -A_0(E)\exp(-\frac{E}{k_B T_c}) + A_1 E^{-1/2} \quad (\text{* MERGEFORMAT 1})$$

PSC Device fabrication and characterization.

The 2.1 cm × 2.1 cm ITO-coated glass substrates were cleaned by sonication in acetone, IPA and ethanol subsequently for 30 min each, followed by ultraviolet-ozone treatment for 20 min. The commercially purchased SnO_2 was mixed with deionized water according to the volume ratio of 1:3, and the mixed solution was oscillated for 1min to obtain the SnO_2 aqueous solution needed for our experiment. SnO_2 solution was spin-coated onto clean glass slides at 3000 rpm for 30 s and then annealed, yielding the resultant film with an electron acceptor. The preparation of perovskite was the same as that of thin film preparation. Then, the 2,2 ,7,7 -tetrakis(N,N-di-p-methoxyphenylamine)-9,90-spirobifluorene (spiro-OMeTAD) solution was spin-coated onto the perovskite film at 3000 rpm for 25 s. Finally, 100 nm silver was thermally evaporated under 3×10^{-4} Pa. PSC devices J-V measurements were carried out

in nitrogen-filled glove box. The devices were measured both in forward scan (1.2 V→ -0.1 V, step 0.01 V).

DFT Calculation

In the Density Functional Theory (DFT) calculations, structural optimizations were carried out within the framework of the generalized gradient approximation (GGA), using the Perdew-Burke-Ernzerhof (PBE) functional [1] implemented in the Vienna *Ab-initio* Simulation Package (VASP) [2,3]. The projector augmented-wave (PAW) method [4,5] was adopted to describe the interactions between ion cores and valence electrons. A plane-wave cutoff energy of 450 eV was set as a fixed parameter throughout the calculations. Van der Waals interactions were taken into account by employing Grime's DFT-D3 method [6,7]. For the self-consistent field (SCF) calculations, a convergence energy threshold of 10^{-5} eV was applied to ensure the accuracy of the results. The equilibrium geometries and lattice constants were optimized until the maximum residual force acting on each atom was reduced to within 0.02 eV·Å^{-1}. During the structural relaxation process, a 2 × 2 × 2 Gamma-centered k-point grid was used to sample the Brillouin zone. Additionally, spin-polarized calculations were performed for all the simulations reported herein.

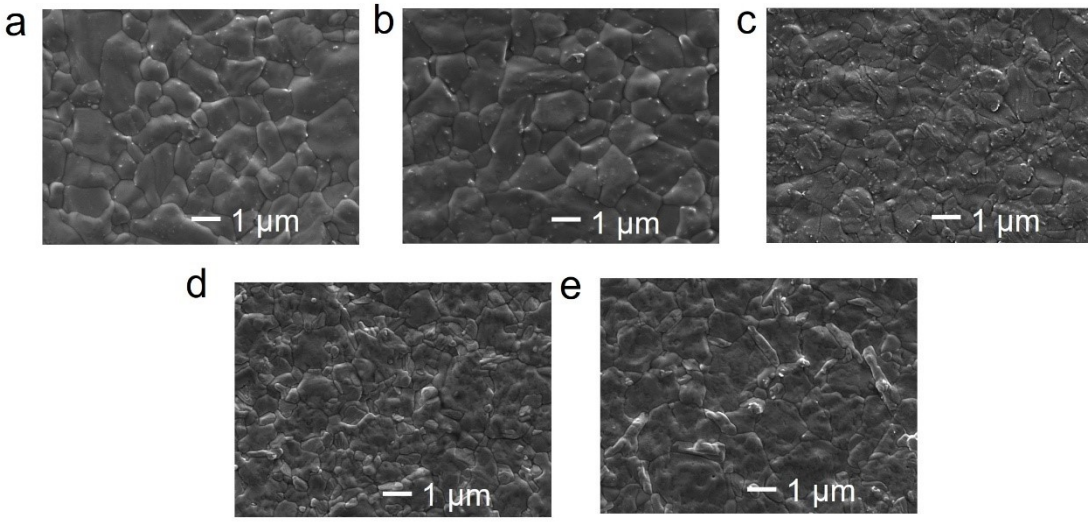

Figure S1. SEM images of (a) $FAPbI_3$-1M, (b) $FAPbI_3$-1.25M, (c) $FAPbI_3$-1.5M, (d) $FAPbI_3$-1.75M and (e) $FAPbI_3$-2M.

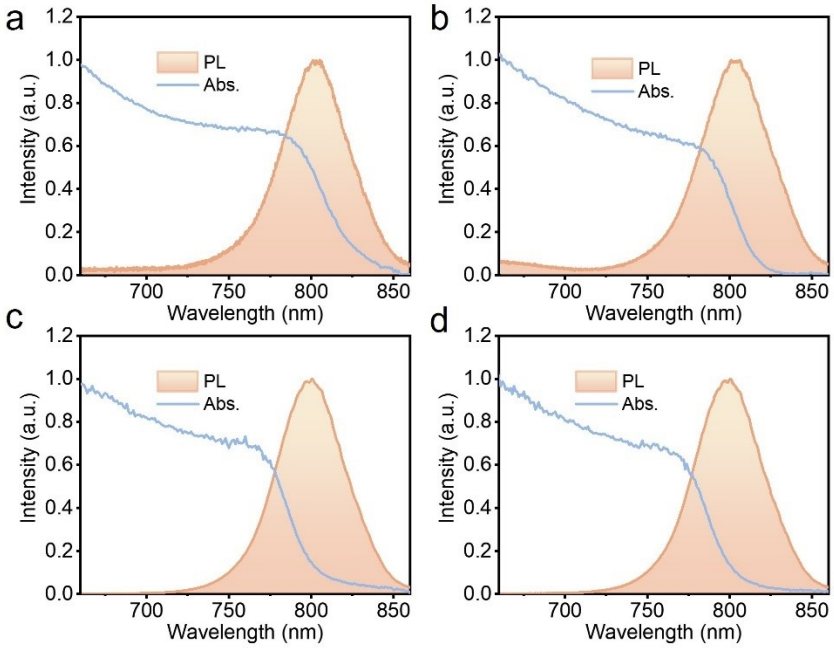

Figure S2. UV-vis absorption and PL spectra of $FAPbI_3$ film: (a) $FAPbI_3$-1M, (b) $FAPbI_3$-1.25M, (c) $FAPbI_3$-1.75M, and (d) $FAPbI_3$-2M.

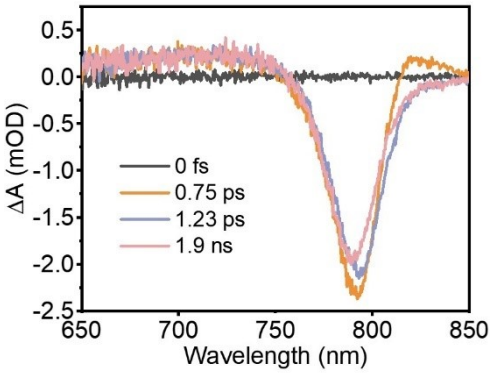

Figure S3. The TA spectra of $FAPbI_3$-1.5M under 400 nm excitation at a fluence of 0.1 $\mu J/cm^2$.

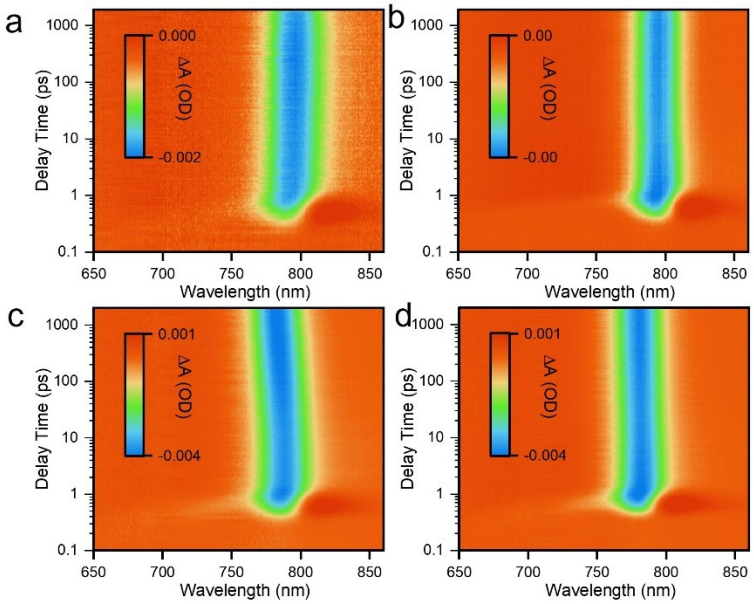

Figure S4. Two-dimensional pseudo color images of TA spectra under 400 nm excitation at a low fluence of 0.1 $\mu J/cm^2$ for various $FAPbI_3$ film: (a) $FAPbI_3$-1M, (b) $FAPbI_3$-1.25M, (c) $FAPbI_3$-1.75M, and (d) $FAPbI_3$-2M.

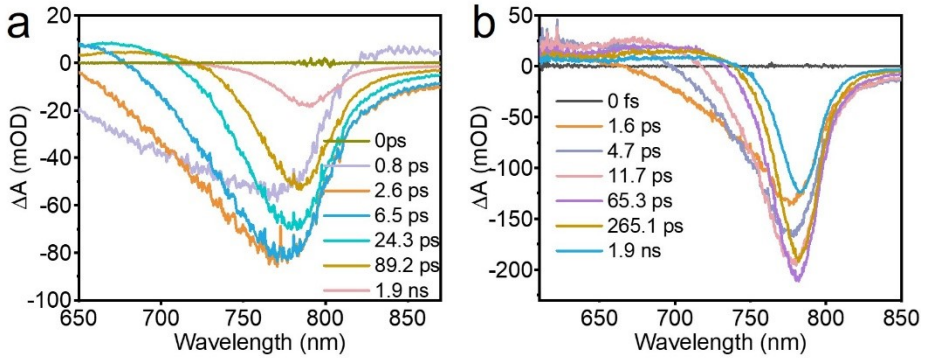

Figure S5. The TA spectra of (a) $FAPbI_3$-1M and (b) $FAPbI_3$-1.5M under 400 nm excitation at a fluence of 33.4 μJ/cm^2.

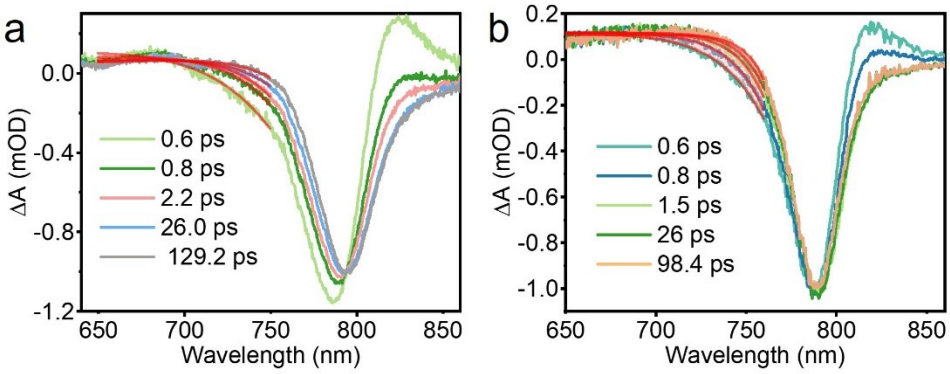

Figure S6. TA spectra with their corresponding Boltzmann distribution fits to the high-energy tail region for (a) $FAPbI_3$-1 M and (b) $FAPbI_3$-1.5 M at low excitation fluence of 1.0 μJ/cm^2.

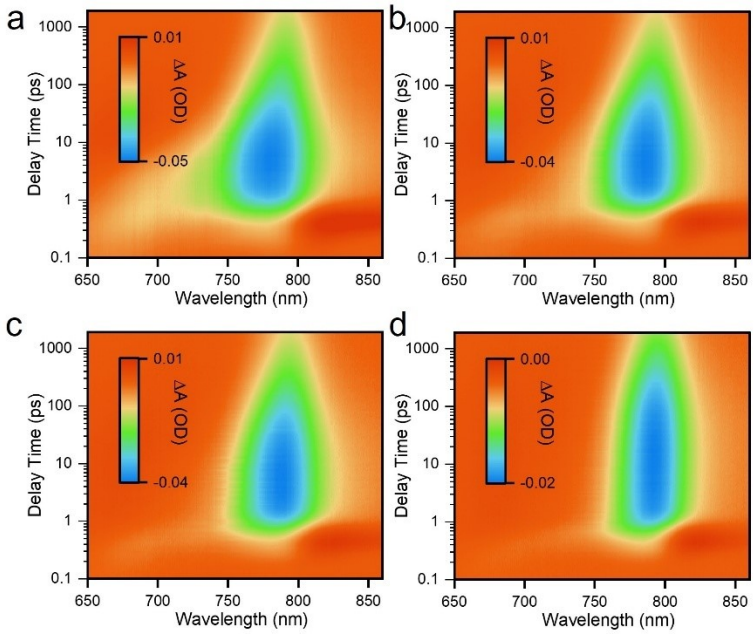

Figure S7. Two-dimensional pseudo color images of TA spectra of $FAPbI_3$-1M under 400 nm excitation at indicated fluence of (a) 31.5 μJ/cm^2, (b) 16.0 μJ/cm^2, (c) 6.4 μJ/cm^2, and (d) 1.0 μJ/cm^2.

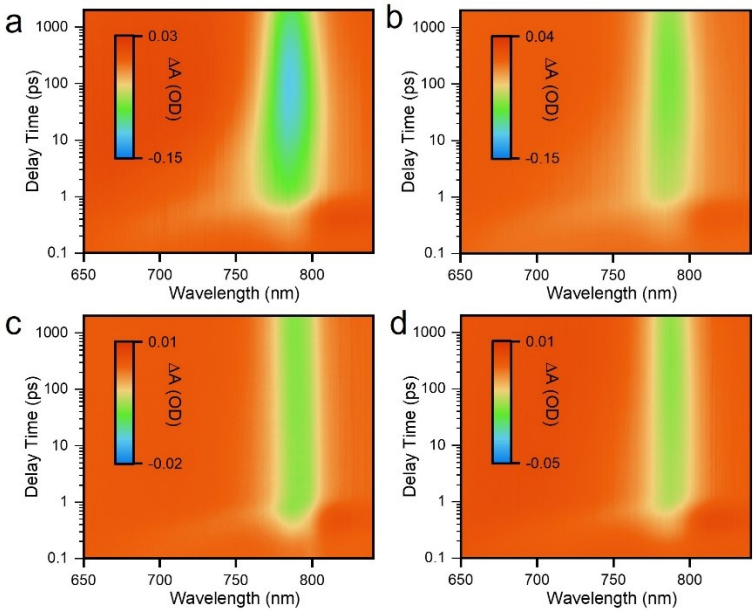

Figure S8. Two-dimensional pseudo color images of TA spectra of $FAPbI_3$-1.5M under 400 nm excitation at indicated fluence of (a) 7.8 μJ/cm^2, (b) 4.1 μJ/cm^2, (c) 1.4 μJ/cm^2, and (d) 1.0 μJ/cm^2.

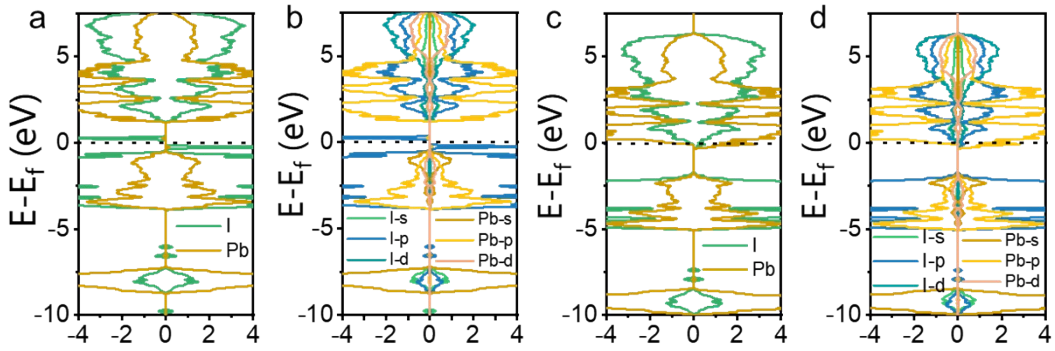

Figure S9. The calculated (a) total density of states (DOS) and (b) projected density of states (PDOS) for interstitial iodine (I_I). The calculated (c) DOS and (d) PDOS for iodine vacancies (V_I).

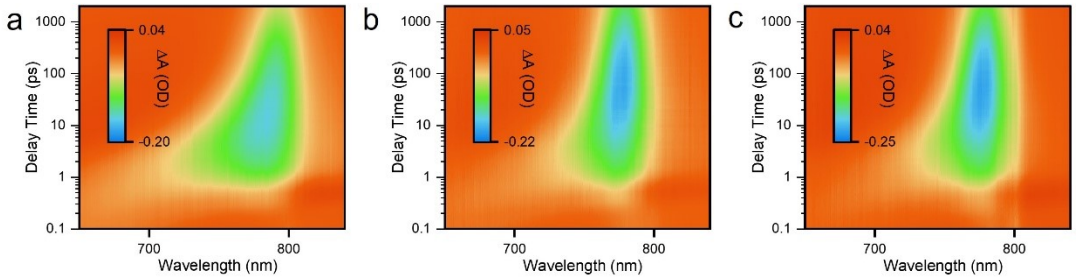

Figure S10. Two-dimensional pseudo color images of TA spectra under 400 nm excitation at a high fluence of 33.4 μJ/cm^2 for (a) $FAPbI_3$-1.25M, (b) $FAPbI_3$-1.75M and (c) $FAPbI_3$-2M.

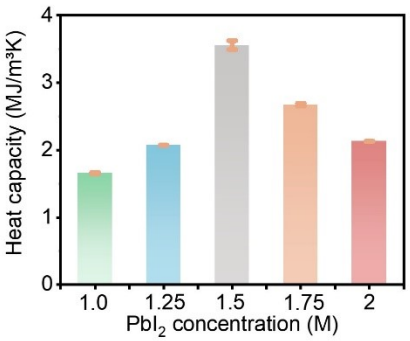

Figure S11. Measured heat capacity of various $FAPbI_3$ films prepared with different concentrations of PbI_2.

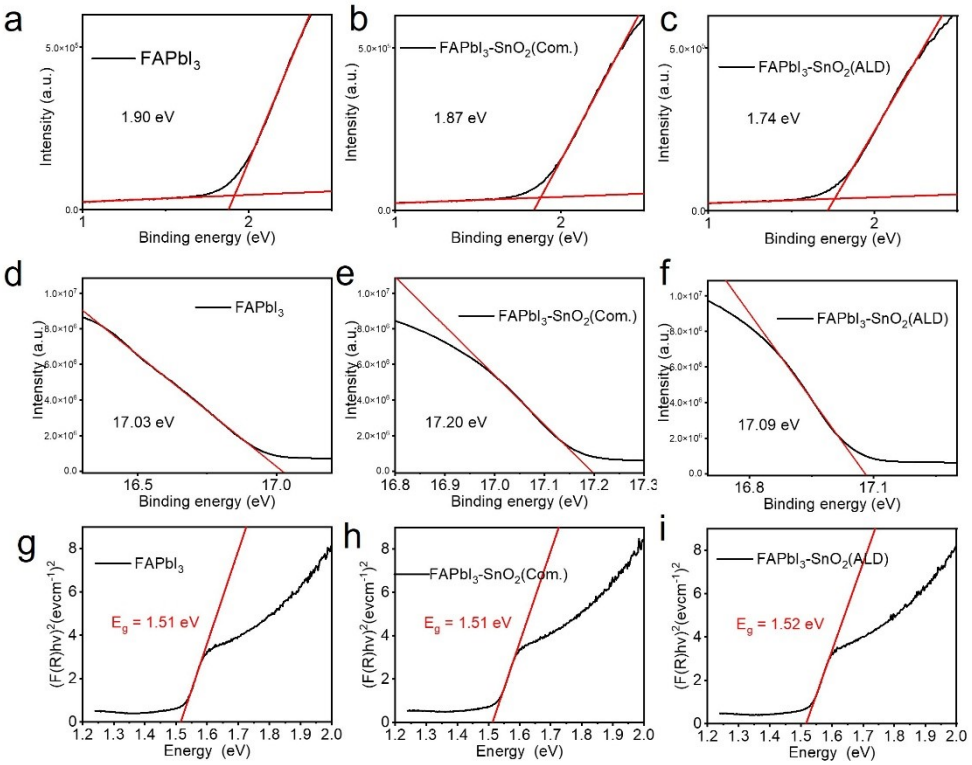

Figure S12. The energy level structures of $FAPbI_3$ perovskite deposited on various electron acceptors determined by UPS and UV-vis spectra. (a)-(c) low binding energy side showing the binding energy between the Fermi level and VBM. (d)-(f) high binging energy side showing the cut-off energies to determine the work function (Fermi level). (g)-(i) bandgap (E_g) calculation derived from UV-vis spectra using the Kubelka-Munk method.

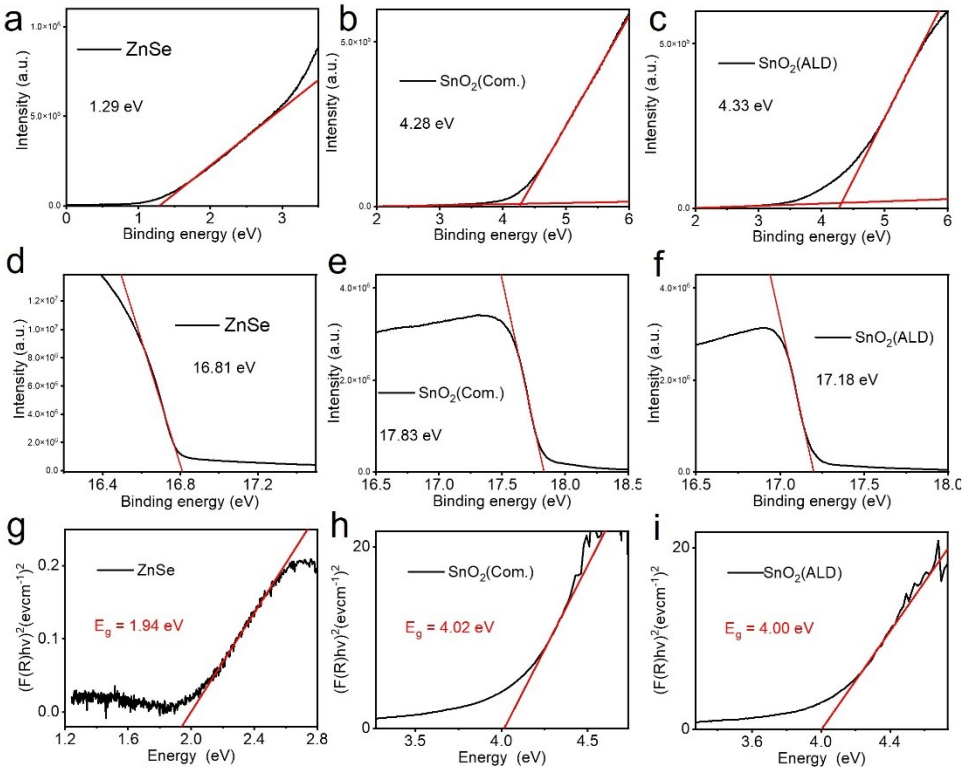

Figure S13. The energy level structures of different electron acceptors determined by UPS and UV-vis absorption spectra. (a)-(c) low binding energy side showing the binding energy between the Fermi level and VBM. (d)-(f) high binging energy side showing the cut-off energies to determine the work function (Fermi level). (g)-(i) Bandgap (E_g) calculation derived from UV-vis spectra using the Kubelka-Munk method.

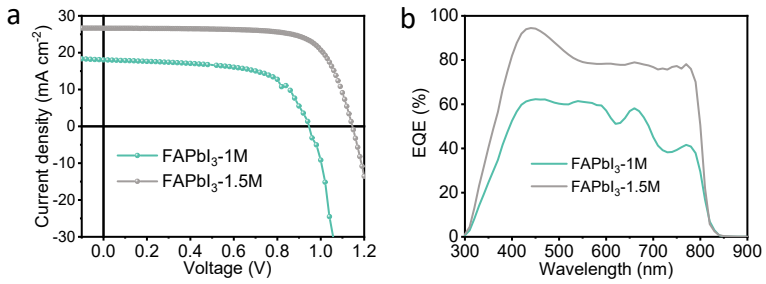

Figure S14. (a) J-V curves of $FAPbI_3$-1 M and $FAPbI_3$-1.5 M by forward scan. (b) EQE spectra of $FAPbI_3$-1 M and $FAPbI_3$-1.5 M.

References

1. Perdew, J. P.; Burke, K.; Ernzerhof, M. Generalized Gradient Approximation Made Simple. Phys. Rev. Lett. 1996, 77, 3865-3868.
2. W. Kohn and L. J. Sham, Phys. Rev., 1965, 140, A1133-A1138.
3. P. Raybaud, J. Hafner, G. Kresse, S. Kasztelan and H. Toulhoat, J. Catal., 2000, 189, 129-146.
4. Kresse, G.; Joubert, D. From Ultrasoft Pseudopotentials to the Projector Augmented-Wave Method. Phys. Rev. B 1999, 59, 1758-1775.
5. Blöchl, P. E. Projector Augmented-Wave Method. Phys. Rev. B 1994, 50, 17953-17979.
6. S. Grimme, J. Antony, S. Ehrlich and H. Krieg, J. Chem. Phys., 2010, 132, 154104.
7. S. Grimme, S. Ehrlich and L. Goerigk, J. Comput. Chem., 2011, 32, 1456-1465.